

Geophysical Research Letters

RESEARCH LETTER

10.1029/2019GL084201

Key Points:

- Accumulation and release of magnetic flux in the middle Jovian magnetosphere modulate auroral intensifications
- Magnetic reconnection process occurs independently of Jupiter's global loading and unloading of magnetic flux
- We provide direct evidence that unloading of magnetic flux causes enhancements of auroral kilometric emissions

Correspondence to:

Z. H. Yao,
zhonghua.yao@uliege.be

Citation:

Yao, Z. H., Grodent, D., Kurth, W. S., Clark, G., Mauk, B. H., Kimura, T., et al. (2019). On the relation between Jovian aurorae and the loading/unloading of the magnetic flux: Simultaneous measurements from Juno, Hubble Space Telescope, and Hisaki. *Geophysical Research Letters*, 46, 11,632–11,641. <https://doi.org/10.1029/2019GL084201>

Received 7 JUL 2019























Accepted 13 SEP 2019

Accepted article online 15 OCT 2019

Published online 5 NOV 2019

©2019. American Geophysical Union.
All Rights Reserved.

On the Relation Between Jovian Aurorae and the Loading/Unloading of the Magnetic Flux: Simultaneous Measurements From Juno, Hubble Space Telescope, and Hisaki

Z. H. Yao^{1,2} , D. Grodent² , W. S. Kurth³ , G. Clark⁴ , B. H. Mauk⁴ , T. Kimura⁵ , B. Bonfond² , S.-Y. Ye³ , A. T. Lui⁴ , A. Radioti² , B. Palmaerts² , W. R. Dunn⁶ , L. C. Ray⁷ , F. Bagenal⁸ , S. V. Badman⁷ , I. J. Rae⁶ , R. L. Guo² , Z. Y. Pu⁹ , J.-C. Gérard¹, K. Yoshioka¹⁰ , J. D. Nichols¹¹ , S. J. Bolton¹² , and S. M. Levin¹³ 

¹Now at Key Laboratory of Earth and Planetary Physics, Institute of Geology and Geophysics, Chinese Academy of Sciences, Beijing, China, ²Laboratoire de Physique Atmosphérique et Planétaire, STAR Institute, Université de Liège, Liège, Belgium, ³Department of Physics and Astronomy, University of Iowa, Iowa City, IA, USA, ⁴Applied Physics Laboratory, Johns Hopkins University, Laurel, MD, USA, ⁵Frontier Research Institute for Interdisciplinary Sciences, Tohoku University, Sendai, Japan, ⁶University College London, Mullard Space Science Laboratory, Dorking, UK, ⁷Department of Physics, Lancaster University, Bailrigg, Lancaster, UK, ⁸Laboratory for Atmospheric and Space Physics, University of Colorado Boulder, Boulder, CO, USA, ⁹School of Earth and Space Sciences, Peking University, Beijing, China, ¹⁰Department of Complexity Science and Engineering, University of Tokyo, Kashiwa, Japan, ¹¹Department of Physics and Astronomy, University of Leicester, Leicester, UK, ¹²Southwest Research Institute, San Antonio, TX, USA, ¹³Jet Propulsion Laboratory, Pasadena, CA, USA

Abstract We present simultaneous observations of aurorae at Jupiter from the Hubble Space Telescope and Hisaki, in combination with the in situ measurements of magnetic field, particles, and radio waves from the Juno Spacecraft in the outer magnetosphere, from $\sim 80R_J$ to $60R_J$ during 17 to 22 March 2017. Two cycles of accumulation and release of magnetic flux, named magnetic loading/unloading, were identified during this period, which correlate well with electron energization and auroral intensifications. Magnetic reconnection events are identified during both the loading and unloading periods, indicating that reconnection and unloading are independent processes. These results show that the dynamics in the middle magnetosphere are coupled with auroral variability.

1. Introduction

Jupiter produces the most powerful auroral emissions among the solar system's planets. Jovian ultraviolet aurora is composed of at least four distinctive components, for example, Galilean satellite magnetic footprints, main auroral emission (Clarke et al., 2002), emissions equatorward and poleward of the main auroral emission (Grodent, 2015, and references therein). These auroral components do not behave fully independently. Grodent et al. (2018) suggested six families of auroral morphologies with diverse combinations of different auroral components by examining 118 observing sequences using the Hubble Space Telescope (HST) between Juno orbits 3 to 7, demonstrating that different auroral components are systematically connected. The Jovian auroral components are highly variable and traditionally thought to be driven by rapid planetary rotation and the Io plasma torus (Clarke et al., 2004; Delamere, Bagenal, et al., 2015; Khurana et al., 2004). Observations of the solar wind upstream of Jupiter by the Juno and Jovian polar FUV emission by HST (or simultaneous measurements by Cassini and Galileo during the Cassini flyby) confirmed that solar wind conditions significantly modulate polar auroral emissions (Clarke et al., 2009; Gurnett et al., 2002; Nichols et al., 2007; 2017). In addition to UV emission, solar wind influences on Jovian aurorae at other wavebands, for example, infrared emissions (Baron et al., 1996; Connerney & Satoh, 2000; Moore et al., 2017) and X-ray emissions (Dunn et al., 2016).

Unlike the terrestrial magnetospheric processes that are mainly driven by Dungey cycle (Dungey, 1961), Jupiter's magnetospheric processes are driven by both Dungey cycle and Vasyliunas cycle (Vasyliunas, 1983). Although energy and plasma sources are fundamentally different at the two planets, previous studies have revealed that many terrestrial-like dynamics could also exist in Jovian magnetosphere (Cowley et al.,

2003). Episodes of magnetic loading processes, corresponding to the substorm growth phase at Earth, have been identified in the near Jovian magnetotail by Galileo (Ge et al., 2007). Furthermore, magnetic reconnection has also been reported in the middle to outer Jovian magnetosphere (Ge et al., 2010; Russell et al., 1998) and suggested to be a mechanism releasing the magnetotail energy (Kasahara et al., 2013; Kronberg et al., 2005, 2008; Vogt et al., 2010, 2014). Previous studies also revealed strong connection between bursts of auroral radio flux and energetic magnetospheric events, which are suggested to relate to plasma instabilities or plasma injections from the more distant magnetodisc (Louarn et al., 2000), or between auroral radio flux and ultraviolet (UV) auroral emissions (Kurth et al., 2005), suggesting that radio emissions are concurrent phenomena during magnetic unloading processes (Louarn et al., 2001). Unlike imaging of the UV aurorae that provides an almost global view, auroral radio flux heavily depends on the viewing geometry, which makes it difficult to distinguish between spatial and temporal variations. Therefore, the analysis of measurements combining data sets from radio waves, energetic particles, magnetic field, and aurorae is pivotal in understanding how the Jovian magnetospheric dynamics drive the polar auroral emissions.

Using simultaneous remote sensing of aurorae from HST and Hisaki, in combination with measurements from Juno in the outer magnetosphere at $\sim 60\text{--}80R_J$, we report direct evidence of the connection between auroral enhancements and unloading of magnetic flux. We also discuss the relation between magnetic reconnection and the loading/unloading process.

2. Observations

Figure 1 (top panel) shows polar projections of five auroral images averaged over ~ 40 min. These images were taken by HST/STIS during 17 to 21 March 2017 (details described in Grodent et al., 2018). The power of the total visible area from HST from 17 to 21 March are 2068 GW, 1778 GW, 2258 GW, 1672 GW, and 1281 GW, respectively. Note that the viewing geometry for these HST sequences is very similar, so that the geometric influence in the comparison would not likely seriously affect the trend of auroral power variation. As illustrated by the auroral power and also visually identifiable by eyes, the aurorae on 17 and 19 March were more brightened than on other days, particularly on the dawn side auroral arc. On 21 March, the auroral emission was significantly weaker than the other images, suggesting a relative quiet magnetospheric condition. Figure 1 (bottom panel) shows the solar wind dynamic pressure at Jupiter using a one-dimensional magnetohydrodynamic model to propagate solar wind measurements made at the Earth orbit (Tao et al., 2005). The Earth-Sun-Jupiter angle was about 40° (not shown), smaller than the threshold in Tao et al., 2005 (i.e., 50°), suggesting that the prediction is relatively reliable with a maximum error of 2 days. As shown in the Tao model prediction, a rapid dynamic pressure enhancement was observed at the beginning of 18 March, followed with a peak value of ~ 0.3 nPa. Although we could not determine the exact arrival time of solar wind compression using a propagation model, it is likely that the enhanced auroral sequences from 17 to 20 March were associated with this strong solar wind dynamic pressure estimated from Tao model.

During the same period, the Juno spacecraft was approaching Jupiter from $84.3R_J$ on 17 March to $59.5R_J$ on 22 March on the dawnside (local time at ~ 4.8), near the equatorial plane. Figures 2a–2c show 1-min averaged measurements of the magnetic field components in system III coordinate system, obtained from the Juno's Magnetometer Investigation (Connerney et al., 2017). Figure 2d shows the 10-hr averaged total magnetic strength, which eliminates the short timescale fluctuations, for example, at timescales of minutes to a few hours. During Juno's pass through Jupiter's outer to middle magnetosphere, the 10-hr flapping of the current sheet caused by planetary rotation leads to regular current sheet crossings that can be identified by the oscillation of the B_r and B_ϕ components (Figures 2a and 2c) and electron flux (Figures 2h). Indeed, when Juno travels from outside to inside the plasmadisc, the dominant components (B_r and B_ϕ) decrease, and the normal component (B_θ) increases. Therefore, the magnetic inclination angle (defined as $\tan^{-1} \left| \frac{B_\theta}{\sqrt{B_r^2 + B_\phi^2}} \right|$) increases accordingly. In a thick current sheet structure, Juno would stay within the central plasmadisc for a relatively long time, and the one-rotation averaged magnetic inclination angle would consequently be larger than in a thin current sheet. We thus suggest using the one-Jovian-rotation average of magnetic inclination angle as an indicator of the current sheet thickness, as shown in Figure 2e. For Earth, the magnetic inclination is often directly used as an indicator of the current sheet thickness (or magnetic

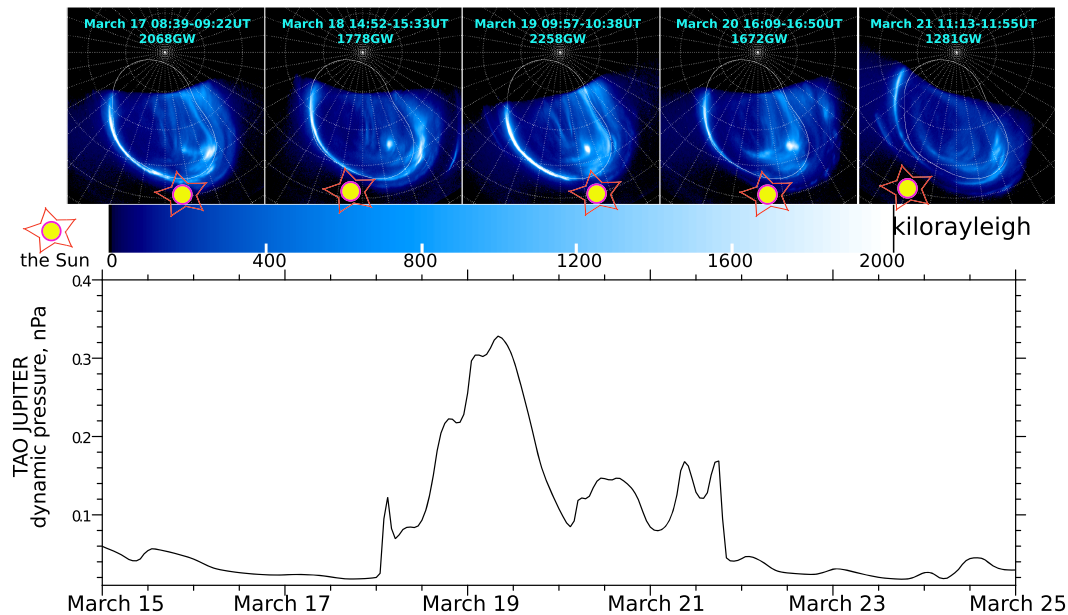


Figure 1. Top: Polar projections of five auroral images from 17 March to 21 March 2017. Each auroral image was averaged over ~40 min. Bottom: The solar wind dynamic pressure was obtained using the 1-D magnetohydrodynamic model available through CDP/AMDA tool via <http://amda.irap.omp.eu>, which was initially developed by Tao et al. (2005).

dipolarization); however, this is not applicable for Jupiter or Saturn because current sheet flapping is modulated by planetary rotation (e.g., Henderson et al., 2006). Figure 2f shows a frequency-time spectrogram of electric field spectral density from the kilometric wave frequencies measured with the Juno-Waves instrument (Kurth, Imai, et al., 2017). Figure 2g shows the wave power intensity of ~60-kHz emissions as a function of time and system III longitude. We select ~60 kHz only for demonstrating the longitude information for the wave activity, while not from a physical consideration. Figure 2h shows an energy-time spectrogram for energetic electrons with an energy range between 30 and 1,000 keV observed with Juno's Jupiter Energetic-Particle Detector Instrument (Mauk et al., 2017). The most prominent variation in Figure 2e is the strong enhancement after 19 March (indicated by the arrow), which indicates a strong current sheet expansion. This is also associated with a strong enhancement of kilometric emission as shown in Figure 2f and electron energization appearing in Figure 2h. The enhancement of energetic electrons lasted for about two planetary rotations, indicating that this is a global process, rather than a localized energization. A localized energization in a rotating magnetosphere would likely result in short duration enhancement with clear boundaries, for example, Yao et al. (2018).

As indicated by the dashed red and orange lines in Figure 2d, the 10-hr averaged $|B|$ has experienced two increases and two decreases during the 5 days, suggesting that the magnetosphere was experiencing loading and unloading of magnetic energy. Note here that we do not focus on the subscale variations caused by current sheet distortion, for example, during the second unloading period, when the magnetic field and electron flux are highly perturbed. When mirroring the dashed lines on Figure 2d to the Figure 2h, it is obvious that the unloading and loading processes are generally consistent with electron energization and cooling, respectively. We point out that the transitions between the loading and unloading processes (marked by the orange and red dashed lines) cannot be temporally resolved finer than one planetary rotation; therefore, we cannot conclude whether or not there exists a small time delay between the magnetic variation and the electron energization. We mark the times of the five auroral images in Figure 1 on the top of Figure 2a (purple arrows), and coincidentally the images sampled all the four periods of the unloading and loading processes. The two enhanced auroral emissions (17 and 19 March) were observed at the beginning of the unloading processes (indicated in Figure 2d), while the three relatively faint auroral emissions (18, 20, and 21 March) occurred during the loading processes.

During this current sheet expansion, the auroral kilometric wave power (Figure 2f) significantly increased and showed strong planetary rotation modulation. Ladreiter et al. (1994) show that both hectometric

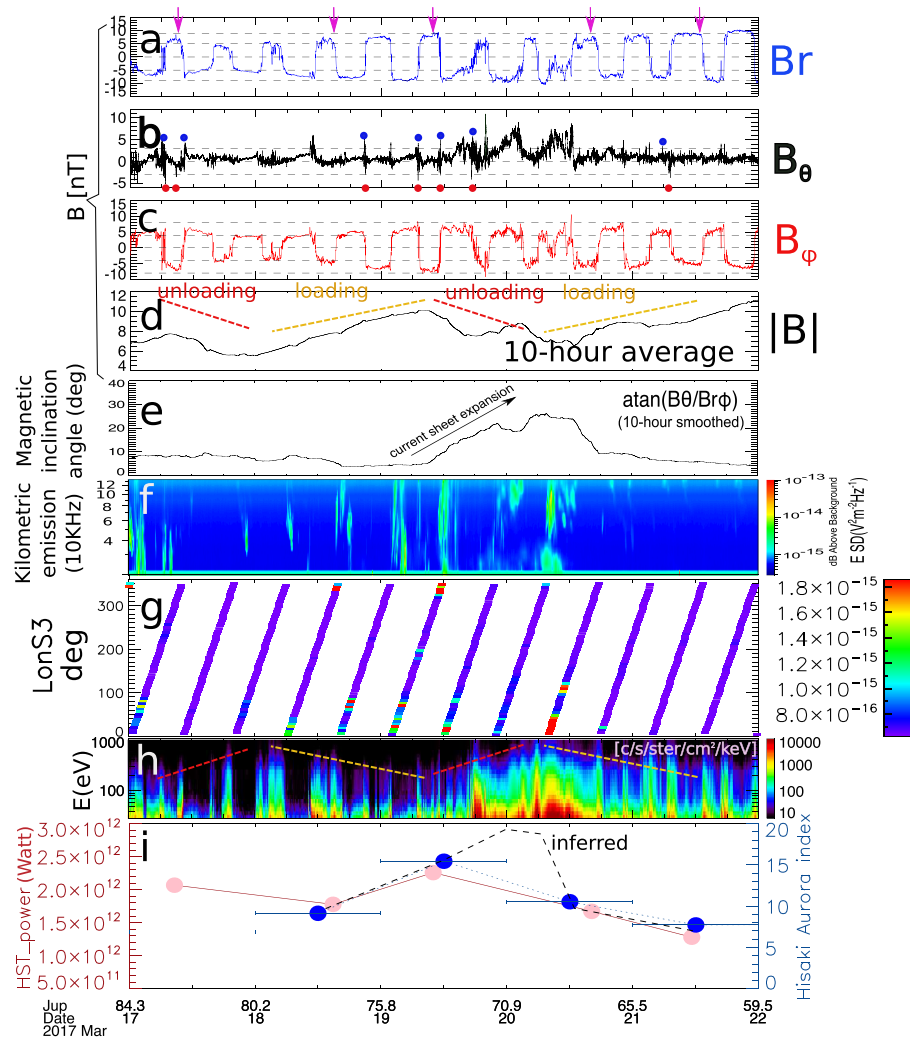


Figure 2. (a–c) The 1-min averaged magnetic field components in system III measured by the Juno-Magnetometer Investigation instrument; (d) 10-hr averaged magnetic strength; (e) 10-hr averaged magnetic inclination angle, defined as $\tan^{-1} \left| \frac{B_\theta}{\sqrt{B_r^2 + B_\phi^2}} \right|$; (f) frequency-time spectrograms of electric field spectral density;

(g) the wave power intensity of ~ 60 -kHz emissions as a function of time and system III longitude; (h) energetic electrons measured by the Juno Jupiter Energetic-particle Detector Instrument; and (i) index of total auroral power from Hisaki (blue) and total auroral power from HST (pink). The Hisaki auroral index was derived from 1-day averaged measurements as indicated by the horizontal bars centered at each data point. The red dots on the top of (b) indicate negative spikes of B_θ . The blue dots in (b) mark positive B_θ spikes that might be closely related to the negative B_θ spikes. The purple arrows on the top of (a) indicate the times of the five HST images in Figure 1a. The dashed curve in (i) is a potential variation inferred from HST, Hisaki, and kilometric emissions.

(HOM) and broadband kilometric (bKOM) emissions are associated with auroral activities and further suggest that bKOM is likely associated with outer magnetosphere while HOM is likely to be connected with inner Jovian plasma sheet and/or outer plasma torus. Furthermore, Louarn et al. (2014) reveal the correlation between narrow-band kilometric emission (nKOM) and magnetospheric reconfiguration event. In the present study, we do not find either clear nKOM or strong auroral injection. The HOM is not discussed in the present study because of instrument noise interferences at its frequency range (Kurth, Hospodarsky, et al., 2017). Figure 2g shows that the kilometric wave emissions were mostly constrained from ~ 320 – 340° to $\sim 100^\circ$ in system III. The modulation might be due to the magnetic dipole tilt, which causes the radio emission cone to rock in latitude as the planet rotates (Green & Boardsen, 1999; Kurth et al., 2005; Morgan & Gurnett, 1991). Juno only observes radio emission when it intersects the emission cone. So the power modulation might be due to the periodic changes of visibility of kilometric radio emission from Juno. The wave power enhancement in a fixed longitude range in system III coordinates was revealed by measurements from *Voyager 1* and *2* (Kurth et al., 1980) and suggested to be associated

with terrestrial substorm-like activities at Jupiter (i.e., the magnetic unloading process used in the present study) in Jovian magnetosphere. Therefore, the present study provides direct evidence of their hypothesis.

Figure 2i shows the auroral power index from the count rate at 1115 Å measured by Hisaki EXCEED (blue; Yoshioka et al., 2013) and the total auroral power from HST (pink). The Hisaki power variations are reduced from the imaging spectral data produced by the pipeline system described in Kimura et al. (2019), by integrating over 1 day, which filters out rapid variations associated with disturbance in the satellite attitudinal system with timescale smaller than 1 day. The HST auroral power includes HST's total visible area. Both HST and Hisaki show consistent variations, supporting the magnetic loading/unloading modulation of Jovian aurorae and auroral kilometric radiations. We notice that auroral kilometric radiation enhancement lasts for a little bit longer than the auroral indicators from HST and Hisaki observations. Because HST and Hisaki observations are at ~1-day resolution, so that the slight time delay might not be due to physical reason. The inferred dashed black curve could be a potential solution to this slight time delay.

As indicated by the red dots on the bottom of Figure 2b, there are at least seven strong spikes (less than -3 nT) of negative B_{θ} , which is usually taken as an indicator of magnetic reconnection in the Jovian magnetosphere (Kronberg et al., 2005; Russell et al., 1998; Vogt et al., 2010). Moreover, positive B_{θ} spikes, marked by blue dots, are found close to these negative B_{θ} spikes. The pairs of positive and negative spikes imply that the Juno spacecraft traveled into both reconnection outflow sides, meaning that the reconnection sites were likely formed at the spacecraft's location or travelled through the spacecraft (Kasahara et al., 2013; Kronberg et al., 2012), or plasmoid ejected from the reconnection site passed over the spacecraft (Vogt et al., 2014, 2010). When comparing these reconnection signatures with the loading/unloading processes, we found that episodes of reconnection were encountered not only during the magnetic unloading periods but also during the loading periods. These results indicate that magnetic reconnection can behave independently of the magnetic loading/unloading processes in Jupiter's magnetosphere.

3. Discussion and Summary

It is a major challenge to distinguish between spatial and temporal variations from single-probe measurements. Because Juno continuously travels along its 53-day orbit (Bolton et al., 2017), we have an ideal opportunity to compare the active and quiet-time measurements along similar trajectories between the nearby orbits to distinguish between spatial and temporal variations. Figures 3a and 3b show Juno's trajectory (distance to Jupiter's center versus distance above the magnetic equator) in the periods during 17–22 March 2017 (orbit 5) and during 1–6 July 2017 (orbit 7). Figures 3c and 3d are two representative auroral images (the same color scale) for the two periods, showing that the measurements in orbit 5 were made during active aurora period while the measurements in orbit 7 were performed during quiet aurora period. Figures 3e and 3f shows the magnetic strength during the two periods. As we explained in the observations section, the oscillation of magnetic strength is due to planetary rotation induced plasmadisc flapping. When the spacecraft move out of the plasma disk during the plasmadisc flapping, the change of $|B|$ becomes much more gentle. Therefore, we subtract the envelope of $|B|$ using the criterion of $|dB/dt| < 1$ nT/s. This envelope (blue dots) shall generally represent the lobe magnetic field. Figure 3g shows a direct comparison of the lobe magnetic field variations during orbit 5 (the active aurora period) and orbit 7 (the quiet aurora period). Note that the label of distance to Jupiter may involve an inaccuracy of $\sim 1R_J$, as the two orbits were not precisely the same. The lobe magnetic field during orbit 7 gradually increased, representing a trajectory variation. While the lobe magnetic field during orbit 5 shows clear variations along the trajectory variation. It is surprising that during the active auroral period, the lobe magnetic field could drop to the quiet auroral period level. Because we do not have a continual monitor of the polar aurorae, we could not examine whether or not aurora during orbit 5 could transiently reach to the quiet time level. We point out that (1) the magnetic loading/unloading process is in a timescale of one to several planetary rotations, which is much longer than the Alfvén travelling time from the equator to the ionosphere. (2) The correlation of lobe magnetic energy release would result in an inner magnetospheric energy release and auroral brightening, so that the correlation between lobe magnetic variation and aurora would be obtained even when the spacecraft is not magnetically connected to the auroral region (e.g., Angelopoulos et al., 2013).

The relation between magnetic reconnection and loading/unloading processes is an intriguing mystery widely existing in many planetary magnetospheres in the solar system. Although magnetic dipolarization

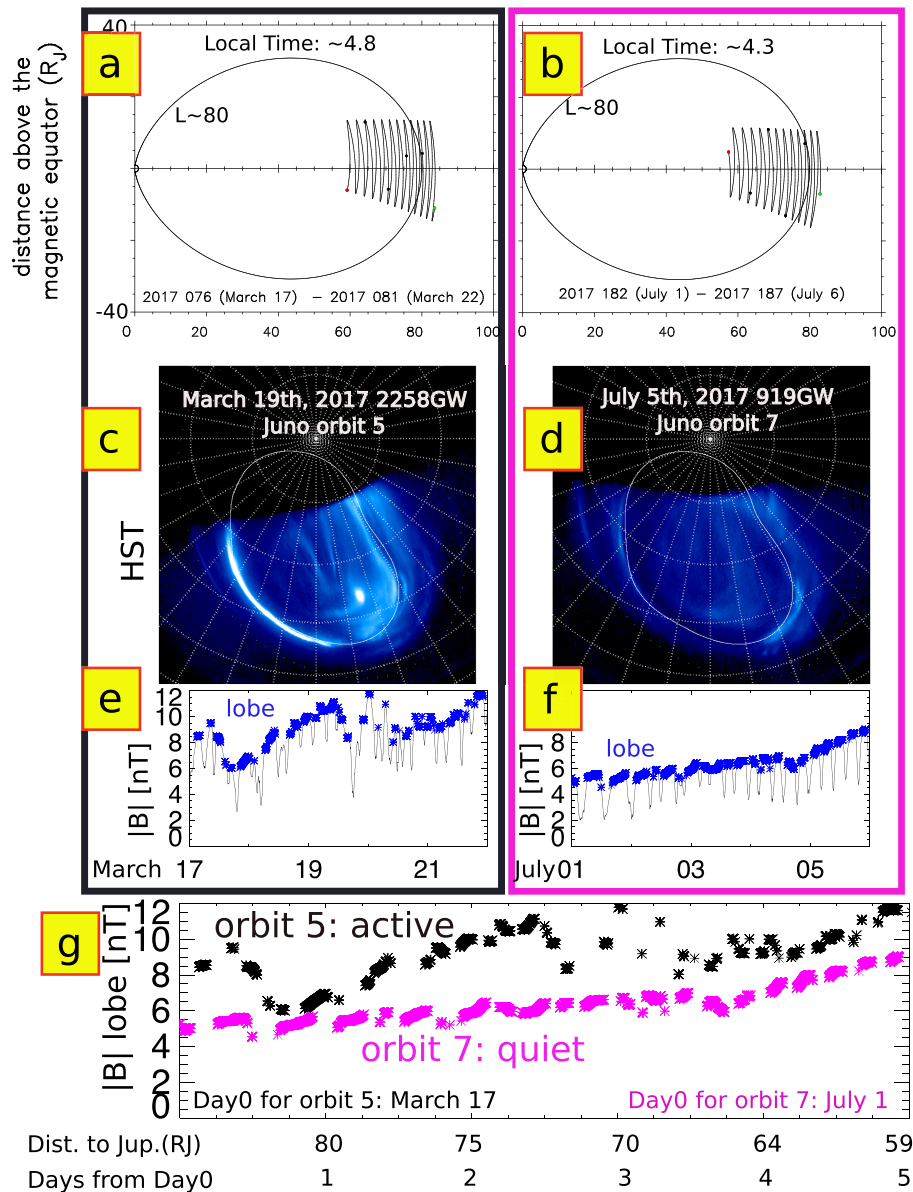


Figure 3. (a, b): Juno's trajectory (distance to Jupiter's center versus distance above the magnetic equator) in the periods during 17–22 March 2017 (orbit 5) and during 1–6 July 2017 (orbit 7). (c, d) Two representative auroral images for the two periods. (e, f) Magnetic strength during the two periods and the envelope of $|B|$ (marked by the blue dots) were obtained using the criterion of $|dB/dt| < 1$ nT/s. (g) The comparison of the lobe magnetic field variations during orbit 5 (the active aurora period, black) and orbit 7 (the quiet aurora period, pink).

and magnetic unloading are the same physical process, the magnetic unloading signatures (decreases of lobe field strength) are measurable at a large range of distances while dipolarization signatures (i.e., increases of magnetic inclination angle or B_θ) are less significant at larger distances from the planet (Angelopoulos et al., 2013; Shukhtina et al., 2014). This is why only the second magnetic unloading was accompanied by a strong increase in the magnetic inclination angle. It is usually suggested that the unloading process is driven by magnetic reconnection at Earth (Angelopoulos et al., 2008), Saturn (Yao, 2017), and Jupiter (Ge et al., 2007; Russell et al., 1998). Conversely, there are also extensive studies revealing that the terrestrial unloading process is not driven by magnetic reconnection from the examination of their timing history (e.g., reconnection occurs after the unloading process; Lui, 2009) and energy budget (Akasofu, 2017; Lui, 2015, 2018). One of the major difficulties in understanding their relation is due to the similar timescales (i.e., several minutes) of terrestrial transient phenomena, such as reconnection, plasma bursty bulk flow,

substorm expansion, and field-aligned current formations. As shown in Figure 2, the loading and unloading processes at Jupiter have timescales of one to a few planetary rotations, which is much longer than the reconnection signatures (the B_{θ} spikes). Here we show that magnetic reconnection processes could occur during both loading and unloading periods in Jupiter's magnetosphere, although the occurrence rate might be higher during unloading (5/7) than the loading phase (2/7). The potentially different reconnection occurrence rate may be related to the 2- to 3-day quasi-periodical polar dawn spots revealed by Radioti et al. (2008). The successive reconnection signatures during several planetary rotations might suggest a drizzle-like reconnection process at Jupiter, which is an analogy to Saturn's drizzle-like reconnection picture proposed by Delamere, Otto, et al. (2015) and supported by direct reconnection evidence (Guo, Yao, Sergis, et al., 2018; Guo, Yao, Wei, et al., 2018). Sporadic reconnections separated by much shorter timescales were also reported by Kronberg et al. (2009). These reconnection signatures measured between 60 to $84R_J$ in this study are also consistent with the inferred X-line in Vogt et al. (2010) and Woch et al. (2002), where they suggest X-line to be located between 60 to $90R_J$ in the postmidnight to the dawn sectors. The appearances of magnetic reconnection at both magnetic loading and unloading phases are also consistent with the statistical conclusion by Vogt et al. (2010).

The loading/unloading of magnetic flux specifically focuses on energy circulation, which is a counterpart of planetary mass circulation (Bagenal & Delamere, 2011; Delamere & Bagenal, 2010; Delamere, Bagenal, et al., 2015). In our point of view, the magnetic loading/unloading process is similar to the process of plasmoid ejection (Cowley et al., 2015; Kronberg et al., 2008; Vogt et al., 2014) and recurrent auroral enhancements in Kimura et al. (2018). Mass loading/unloading is more on the view of global mass circulation, while the magnetic loading/unloading process describes a fundamental process of magnetic energy circulation that involves direct particle energization. The relation between mass loading and magnetic dipolarization is analogous to the relation between terrestrial substorm and solar wind input energy in the magnetosphere, that is, substorm expansion has higher occurrence rate during high solar wind energy input (Newell et al., 2007, 2013). Another relevant analogy is to the process of terrestrial ionospheric outflow in driving periodic magnetic dipolarizations in the terrestrial magnetosphere (Brambles et al., 2010).

The swap between loading and unloading shown in Figure 2 could also fit into the quasiperiodic dynamics of the Jovian magnetosphere revealed by Kronberg et al. (2007) and Louarn et al. (2007). Two complete cycles of the loading and unloading processes were recorded in 5 days, which is highly consistent with the 2.6-day periodic energetic particle bursts in the predawn Jovian magnetotail revealed in Krupp et al. (1998), although Kronberg et al. (2009) summarized that these periodicities could vary from 1 to 7 days. The auroral brightening in this study is likely different from the transient auroral brightening described mainly based on Hisaki data set (Kimura et al., 2017, 2018; Kita et al., 2016). The transient auroral brightenings in their studies are initiated from predawn to dawn local times and rapidly expand in both latitude and longitude over a few hours, which decay in one to two planetary rotations. In contrast, the enhanced auroral morphology remains relatively steady for about 4 days. We note that Ge et al. (2007) suggested the magnetic loading/unloading process to occur at quiet solar wind condition, while it is likely that a similar process occurred during the solar wind compression in this study. We suggest that this event was likely during a solar wind compression based on the auroral morphology suggested by Grodent et al. (2018) and Nichols et al. (2017) owing to enhancements in the main emission and duskside polar region. This is also consistent with the modeled solar wind propagation (Tao et al., 2005). We consider the magnetic loading/unloading process as a fundamental driver of energy conversion between magnetic energy and auroral energy and suggest that this process occurred during a solar wind compression condition (note that we do not suggest a causality between solar wind compression and magnetic loading/unloading), in addition to the previous suggestion that magnetic loading/unloading could occur during a quiet solar wind condition (Ge et al., 2007).

The origin of the magnetosphere-ionosphere coupling currents for the main auroral "oval" in the Jovian system is usually explained as a consequence of the departure of the plasma from rigid corotation in the middle magnetosphere (Cowley & Bunce, 2001; Hill, 1979, 2001). Using measurements from the Galileo magnetometer and plasma wave instrument, Louarn et al. (2016) revealed that the Jovian auroral radio emissions is correlated with the azimuthal component of the magnetic field measured in the plasma disk, which is considered as a supporting evidence for Hill's model (Hill, 1979). The magnetic loading/unloading process described in this study is an independent driver to the corotation enforcement currents. The magnetic loading/unloading process strongly depends on the trends of magnetic variation instead of the absolute

value of magnetic field, that is, growing and decaying of azimuthal and radial components correspond to accumulation (dynamo) and release of magnetic energy (dissipation). We shall also note that the magnetic loading/unloading at $60\text{--}80R_J$ is more distant than the expected magnetospheric origin of the main auroral emission, at $20\text{--}30R_J$ (Cowley & Bunce, 2001; Hill, 2001). We suggest two potential explanations: (1) although the majority of auroral precipitation is at $20\text{--}30R_J$, comparable trends may also exist at $60\text{--}80R_J$. This is also similar to terrestrial auroral intensifications caused by the magnetic unloading process. At Earth, the majority of auroral precipitation comes from ~ 10 Earth radii, while magnetic unloading events are observed at much larger distances (Angelopoulos et al., 2013; Shukhtina et al., 2014), even beyond the reconnection site. (2) There is a current loop between $20\text{--}30R_J$ and $60\text{--}80R_J$, that is, upward currents at $20\text{--}30R_J$, while the downward current branch is formed at $60\text{--}80R_J$. The unloading of magnetic flux at $60\text{--}80R_J$ may correspond to the enhancement of downward currents, which should correspond to an enhanced upward field-aligned currents from 20 to $30R_J$.

Our main results, obtained by combining the 5 days of quasi-continuous remote sensing observations from HST and Hisaki and in situ measurements from the Juno mission, are summarized as follows:

1. The two periods of enhanced auroral emissions were observed when Juno recorded the beginning of the unloading processes, while the three relative diminishing auroral emissions were during the loading processes in the magnetosphere.
2. Kilometric radiation was enhanced during the large magnetic dipolarization process associated with the second unloading phase.
3. Magnetic reconnection appears during both the loading and unloading periods.

References

- Akasofu, S.-I. (2017). Auroral substorms: Search for processes causing the expansion phase in terms of the electric current approach. *Space Science Reviews*, *212*(1-2), 341–381. <https://doi.org/10.1007/s11214-017-0363-7>
- Angelopoulos, V., McFadden, J. P., Larson, D., Carlson, C. W., Mende, S. B., Frey, H., et al. (2008). Tail reconnection triggering substorm onset. *Science*, *321*(5891), 931–935. <https://doi.org/10.1126/science.1160495>
- Angelopoulos, V., Runov, A., Zhou, X.-Z., Turner, D. L., Kiehas, S. A., Li, S.-S., & Shinohara, I. (2013). Electromagnetic energy conversion at reconnection fronts. *Science*, *341*(6153), 1478–1482. <https://doi.org/10.1126/science.1236992>
- Bagenal, F., & Delamere, P. A. (2011). Flow of mass and energy in the magnetospheres of Jupiter and Saturn. *Journal of Geophysical Research*, *116*, A05209. <https://doi.org/10.1029/2010JA016294>
- Baron, R., Owen, T., Connerney, J., Satoh, T., & Harrington, J. (1996). Solar wind control of Jupiter's H^+_3 auroras. *Icarus*, *120*(2), 437–442. <https://doi.org/10.1006/icar.1996.0063>
- Bolton, S., Levin, S., & Bagenal, F. (2017). Juno's first glimpse of Jupiter's complexity. *Geophysical Research Letters*, *44*, 7663–7667. <https://doi.org/10.1002/2017GL074118>
- Brambles, O. J., Lotko, W., Zhang, B., Lyon, J., & Wiltberger, M. J. (2010). Magnetospheric sawtooth oscillations induced by ionospheric outflow. *Science*, *332*(6034), 1183–1186.
- Clarke, J., Ajello, J., Ballester, G., Jaffel, L. B., Connerney, J., Gérard, J.-C., et al. (2002). Ultraviolet emissions from the magnetic footprints of Io, Ganymede and Europa on Jupiter. *Nature*, *415*(6875), 997–1000. <https://doi.org/10.1038/415997a>
- Clarke, J., Nichols, J., Gérard, J. C., Grodent, D., Hansen, K., Kurth, W., et al. (2009). Response of Jupiter's and Saturn's auroral activity to the solar wind. *Journal of Geophysical Research*, *114*, A05210. <https://doi.org/10.1029/2008JA013694>
- Clarke, J. T., Grodent, D., Cowley, S. W., Bunce, E. J., Zarka, P., Connerney, J. E., & Satoh, T. (2004). Jupiter's aurora. In F. Bagenal, T. E. Dowling, W. B. McKinnon (Eds.), *Jupiter: The Planet, Satellites and Magnetosphere* (pp. 639–670). Cambridge, UK: Cambridge University Press.
- Connerney, J., Benn, M., Bjarno, J., Denver, T., Espley, J., Jorgensen, J., et al. (2017). The Juno magnetic field investigation. *Space Science Reviews*, *213*(1-4), 39–138. <https://doi.org/10.1007/s11214-017-0334-z>
- Connerney, J., & Satoh, T. (2000). The H^+_3 ion: A remote diagnostic of the Jovian magnetosphere. *Philosophical Transactions of the Royal Society of London, Series A: Mathematical, Physical and Engineering Sciences*, *358*(1774), 2471–2483. <https://doi.org/10.1098/rsta.2000.0661>
- Cowley, S., & Bunce, E. (2001). Origin of the main auroral oval in Jupiter's coupled magnetosphere–ionosphere system. *Planetary and Space Science*, *49*(10-11), 1067–1088. [https://doi.org/10.1016/S0032-0633\(00\)00167-7](https://doi.org/10.1016/S0032-0633(00)00167-7)
- Cowley, S., Bunce, E., Stallard, T., & Miller, S. (2003). Jupiter's polar ionospheric flows: Theoretical interpretation. *Geophysical Research Letters*, *30*(5), L1220. <https://doi.org/10.1029/2002GL016030>
- Cowley, S. W., Nichols, J., & Jackman, C. (2015). Down-tail mass loss by plasmoids in Jupiter's and Saturn's magnetospheres. *Journal of Geophysical Research: Space Physics*, *120*, 6347–6356. <https://doi.org/10.1002/2015JA021500>
- Delamere, P., & Bagenal, F. (2010). Solar wind interaction with Jupiter's magnetosphere. *Journal of Geophysical Research*, *115*, A10201. <https://doi.org/10.1029/2010JA015347>
- Delamere, P., Bagenal, F., Paranicas, C., Masters, A., Radioti, A., Bonfond, B., et al. (2015). Solar wind and internally driven dynamics: Influences on magnetodiscs and auroral responses. *Space Science Reviews*, *187*(1-4), 51–97. <https://doi.org/10.1007/s11214-014-0075-1>
- Delamere, P., Otto, A., Ma, X., Bagenal, F., & Wilson, R. (2015). Magnetic flux circulation in the rotationally driven giant magnetospheres. *Journal of Geophysical Research: Space Physics*, *120*, 4229–4245. <https://doi.org/10.1002/2015JA021036>
- Dungey, J. W. (1961). Interplanetary magnetic field and the auroral zones. *Physical Review Letters*, *6*(2), 47–48. <https://doi.org/10.1103/PhysRevLett.6.47>

Acknowledgments

Acknowledgements Z. Y. acknowledges the Strategic Priority Research Program of Chinese Academy of Sciences (Grant No. XDA17010201). B. B. is a Research Associate of the Fonds de la Recherche Scientifique-FNRS. Z. Y., D. G., B. P., and J. C. G. acknowledge the financial support from the Belgian Federal Science Policy Office (BELSPO) via the PRODEX Programme of ESA. Z. Y. very much appreciates the fruitful discussion with Dr Krishan Khurana at UCLA, Emmanuel Chané from KU Leuven, Jack Connerney from Goddard Space Flight Center, and Peter Delamere at University of Alaska. The research at the University of Iowa was supported by NASA through contract 699041X with the Southwest Research Institute. L. C. R. was funded by an STFC Consolidated Grant to Lancaster University (ST/R000816/1). W. D. and I. J. R. were funded by an STFC Consolidated Grant to University College London (ST/S000240/1). F. B. was supported by Juno and Hisaki missions. K. Y. acknowledges Grant-in-Aid for Scientific Research (B) 19H01948 funded by JSPS. The auroral images are based on observations with the NASA/ESA Hubble Space Telescope (program HST GO-14634), obtained at the Space Telescope Science Institute (STScI), which is operated by AURA for NASA. All data are publicly available at STScI. All Juno data presented here are publicly available from NASA's Planetary Data System as part of the JNO-J-3-FGM-CAL-V1.0, JNO-J-JED-3-CDR-V1.0, and JNO-E/J/SS-WAV-3-CDR-SRVFULL-V1.0 data sets for the MAG, JEDI, and Waves instruments. We are grateful to JHU/APL's Lawrence E. Brown for his role in developing the core of the data display software used here, and we very much appreciate the Autoplot software that has greatly helped us in processing the Juno/Waves data. The Juno trajectory plot was made via <http://www-pw.physics.uiowa.edu/~jbg/junoplot.html>. The data of Hisaki satellite is archived in the Data Archives and Transmission System (DARTS) JAXA (<https://www.darts.isas.jaxa.jp/stp/hisaki/>). Users can access the data in DARTS directly. T. K. was supported by a Grant-in-Aid for Scientific Research (16K17812) from the Japan Society for the Promotion of Science (JSPS).

- Dunn, W. R., Branduardi-Raymont, G., Elsner, R. F., Vogt, M. F., Lamy, L., Ford, P. G., et al. (2016). The impact of an ICME on the Jovian X-ray aurora. *Journal of Geophysical Research: Space Physics*, *121*, 2274–2307. <https://doi.org/10.1002/2015JA021888>
- Ge, Y., Jian, L., & Russell, C. (2007). Growth phase of Jovian substorms. *Geophysical Research Letters*, *34*, L23106. <https://doi.org/10.1029/2007GL031987>
- Ge, Y., Russell, C., & Khurana, K. (2010). Reconnection sites in Jupiter's magnetotail and relation to Jovian auroras. *Planetary and Space Science*, *58*(11), 1455–1469. <https://doi.org/10.1016/j.pss.2010.06.013>
- Green, J. L., & Boardsen, S. A. (1999). Confinement of nonthermal continuum radiation to low latitudes. *Journal of Geophysical Research*, *104*(A5), 10,307–10,316. <https://doi.org/10.1029/1998JA900130>
- Grodent, D. (2015). A brief review of ultraviolet auroral emissions on giant planets. *Space Science Reviews*, *187*(1–4), 23–50. <https://doi.org/10.1007/s11214-014-0052-8>
- Grodent, D., Bonfond, B., Yao, Z., Gérard, J. C., Radioti, A., Dumont, M., et al. (2018). Jupiter's aurora observed with HST during Juno orbits 3 to 7. *Journal of Geophysical Research: Space Physics*, *123*, 3299–3319. <https://doi.org/10.1002/2017JA025046>
- Guo, R., Yao, Z., Sergis, N., Wei, Y., Mitchell, D., Roussos, E., et al. (2018). Reconnection acceleration in Saturn's dayside magnetodisk: A multicase study with Cassini. *The Astrophysical Journal Letters*, *868*(2), L23. <https://doi.org/10.3847/2041-8213/aadab>
- Guo, R., Yao, Z., Wei, Y., Ray, L. C., Rae, I., Arridge, C. S., et al. (2018). Rotationally driven magnetic reconnection in Saturn's dayside. *Nature Astronomy*, *2*, 640–645. <https://doi.org/10.1038/s41550-018-0461-9>
- Gurnett, D., Kurth, W., Hospodarsky, G., Persoon, A., Zarka, P., Lecacheux, A., et al. (2002). Control of Jupiter's radio emission and aurorae by the solar wind. *Nature*, *415*(6875), 985–987. <https://doi.org/10.1038/415985a>
- Henderson, M., Skoug, R., Donovan, E., Thomsen, M., Reeves, G., Denton, M. H., et al. (2006). Substorms during the 10–11 August 2000 sawtooth event. *Journal of Geophysical Research*, *111*, A06206. <https://doi.org/10.1029/2005JA011366>
- Hill, T. (1979). Inertial limit on corotation. *Journal of Geophysical Research*, *84*(A11), 6554–6558. <https://doi.org/10.1029/JA084iA11p06554>
- Hill, T. (2001). The Jovian auroral oval. *Journal of Geophysical Research*, *106*(A5), 8101–8107. <https://doi.org/10.1029/2000JA000302>
- Kasahara, S., Kronberg, E., Kimura, T., Tao, C., Badman, S., Masters, A., et al. (2013). Asymmetric distribution of reconnection jet fronts in the Jovian nightside magnetosphere. *Journal of Geophysical Research: Space Physics*, *118*, 375–384. <https://doi.org/10.1029/2012JA018130>
- Khurana, K. K., Kivelson, M. G., Vasyliunas, V. M., Krupp, N., Woch, J., Lagg, A., et al. (2004). The configuration of Jupiter's magnetosphere. *Jupiter: The planet, satellites and magnetosphere* (Vol. 1, pp. 593–616). Cambridge, UK: Cambridge University Press.
- Kimura, T., Hiraki, Y., Tao, C., Tsuchiya, F., Delamere, P., Yoshioka, K., et al. (2018). Response of Jupiter's aurora to plasma mass loading rate monitored by the Hisaki satellite during volcanic eruptions at Io. *Journal of Geophysical Research: Space Physics*, *123*, 1885–1899. <https://doi.org/10.1002/2017JA025029>
- Kimura, T., Nichols, J. D., Gray, R., Tao, C., Murakami, G., Yamazaki, A., et al. (2017). Transient brightening of Jupiter's aurora observed by the Hisaki satellite and Hubble Space Telescope during approach phase of the Juno spacecraft. *Geophysical Research Letters*, *44*, 4523–4531. <https://doi.org/10.1002/2017GL072912>
- Kimura, T., Yamazaki, A., Yoshioka, K., Murakami, G., Tsuchiya, F., Kita, H., et al. (2019). Development of ground pipeline system for high-level scientific data products of the Hisaki satellite mission and its application to planetary space weather, edited, EDP Sciences. <https://doi.org/10.1051/swsc/2019005>
- Kita, H., Kimura, T., Tao, C., Tsuchiya, F., Misawa, H., Sakanoi, T., et al. (2016). Characteristics of solar wind control on Jovian UV auroral activity deciphered by long-term Hisaki EXCEED observations: Evidence of preconditioning of the magnetosphere? *Geophysical Research Letters*, *43*, 6790–6798. <https://doi.org/10.1002/2016GL069481>
- Kronberg, E., Glassmeier, K. H., Woch, J., Krupp, N., Lagg, A., & Dougherty, M. (2007). A possible intrinsic mechanism for the quasi-periodic dynamics of the Jovian magnetosphere. *Journal of Geophysical Research*, *112*, A05203. <https://doi.org/10.1029/2006JA011994>
- Kronberg, E., Kasahara, S., Krupp, N., & Woch, J. (2012). Field-aligned beams and reconnection in the jovian magnetotail. *Icarus*, *217*(1), 55–65. <https://doi.org/10.1016/j.icarus.2011.10.011>
- Kronberg, E., Woch, J., Krupp, N., & Lagg, A. (2008). Mass release process in the Jovian magnetosphere: Statistics on particle burst parameters. *Journal of Geophysical Research*, *113*, A10202. <https://doi.org/10.1029/2008JA013332>
- Kronberg, E., Woch, J., Krupp, N., Lagg, A., Khurana, K., & Glassmeier, K. H. (2005). Mass release at Jupiter: Substorm-like processes in the Jovian magnetotail. *Journal of Geophysical Research*, *110*, A03211. <https://doi.org/10.1029/2004JA010777>
- Kronberg, E. A., Woch, J., Krupp, N., & Lagg, A. (2009). A summary of observational records on periodicities above the rotational period in the Jovian magnetosphere. *Annales Geophysicae*, *27*, 2565–2573. <https://doi.org/10.5194/angeo-27-2565-2009>
- Krupp, N., Woch, J., Lagg, A., Wilken, B., Livi, S., & Williams, D. (1998). Energetic particle bursts in the predawn Jovian magnetotail. *Geophysical Research Letters*, *25*(8), 1249–1252. <https://doi.org/10.1029/98GL00863>
- Kurth, W., Hospodarsky, G., Kirchner, D., Mokrzycki, B., Averkamp, T., Robison, W., et al. (2017). The Juno waves investigation. *Space Science Reviews*, *213*(1–4), 347–392. <https://doi.org/10.1007/s11214-017-0396-y>
- Kurth, W., Imai, M., Hospodarsky, G., Gurnett, D., Louarn, P., Valek, P., et al. (2017). A new view of Jupiter's auroral radio spectrum. *Geophysical Research Letters*, *44*, 7114–7121. <https://doi.org/10.1002/2017GL072889>
- Kurth, W. S., Gurnett, D. A., Clarke, J. T., Zarka, P., Desch, M. D., Kaiser, M. L., et al. (2005). An Earth-like correspondence between Saturn's auroral features and radio emission. *Nature*, *433*(7027), 722–725. <https://doi.org/10.1038/nature03334>
- Kurth, W. S., Gurnett, D. A., & Scarf, F. L. (1980). Spatial and temporal studies of Jovian kilometric radiation. *Geophysical Research Letters*, *7*(1), 61–64. <https://doi.org/10.1029/GL007i001p00061>
- Ladreiter, H., Zarka, P., & Lecacheux, A. (1994). Direction finding study of Jovian hectometric and broadband kilometric radio emissions: Evidence for their auroral origin. *Planetary and Space Science*, *42*(11), 919–931. [https://doi.org/10.1016/0032-0633\(94\)90052-3](https://doi.org/10.1016/0032-0633(94)90052-3)
- Louarn, P., Kivelson, M. G., & Kurth, W. S. (2016). On the links between the radio flux and magnetodisk distortions at Jupiter. *Journal of Geophysical Research: Space Physics*, *121*, 9651–9670. <https://doi.org/10.1002/2016JA023106>
- Louarn, P., Kurth, W., Gurnett, D., Hospodarsky, G., Persoon, A., Cecconi, B., et al. (2007). Observation of similar radio signatures at Saturn and Jupiter: Implications for the magnetospheric dynamics. *Geophysical Research Letters*, *34*, L20113. <https://doi.org/10.1029/2007GL030368>
- Louarn, P., Mauk, B., Kivelson, M., Kurth, W., Roux, A., Zimmer, C., et al. (2001). A multi-instrument study of a Jovian magnetospheric disturbance. *Journal of Geophysical Research*, *106*(A12), 29,883–29,898. <https://doi.org/10.1029/2001JA900067>
- Louarn, P., Paranicas, C. P., & Kurth, W. S. (2014). Global magnetodisk disturbances and energetic particle injections at Jupiter. *Journal of Geophysical Research: Space Physics*, *119*, 4495–4511. <https://doi.org/10.1002/2014JA019846>

- Louarn, P., Roux, A., Perraut, S., Kurth, W. S., & Gurnett, D. A. (2000). A study of the Jovian “energetic magnetospheric events” observed by Galileo: Role in the radial plasma transport. *Journal of Geophysical Research*, *105*(A6), 13,073–13,088. <https://doi.org/10.1029/1999JA900478>
- Lui, A. (2009). Comment on “Tail Reconnection Triggering Substorm Onset”. *Science*, *324*(5933), 1391. <https://doi.org/10.1126/science.1167726>
- Lui, A. (2015). Dipolarization fronts and magnetic flux transport. *Geoscience Letters*, *2*(1), 15. <https://doi.org/10.1186/s40562-015-0032-1>
- Lui, A. (2018). Review on the characteristics of the current sheet in the Earth’s magnetotail. *Electric Currents in Geospace and Beyond*, *235*, 155–175. <https://doi.org/10.1002/9781119324522.ch10>
- Mauk, B., Haggerty, D., Jaskulek, S., Schlemm, C., Brown, L., Cooper, S., et al. (2017). The Jupiter Energetic Particle Detector Instrument (JEDI) investigation for the Juno mission. *Space Science Reviews*, *213*(1–4), 289–346. <https://doi.org/10.1007/s11214-013-0025-3>
- Moore, L., O’Donoghue, J., Melin, H., Stallard, T., Tao, C., Zieger, B., et al. (2017). Variability of Jupiter’s IR H₃⁺ aurorae during Juno approach. *Geophysical Research Letters*, *44*, 4513–4522. <https://doi.org/10.1002/2017GL073156>
- Morgan, D., & Gurnett, D. A. (1991). The source location and beaming of terrestrial continuum radiation. *Journal of Geophysical Research*, *96*(A6), 9595–9613. <https://doi.org/10.1029/91JA00314>
- Newell, P., Gjerloev, J., & Mitchell, E. (2013). Space climate implications from substorm frequency. *Journal of Geophysical Research: Space Physics*, *118*, 6254–6265. <https://doi.org/10.1002/jgra.50597>
- Newell, P., Sotirelis, T., Liou, K., Meng, C. I., & Rich, F. (2007). A nearly universal solar wind-magnetosphere coupling function inferred from 10 magnetospheric state variables. *Journal of Geophysical Research*, *112*, A01206. <https://doi.org/10.1029/2006JA012015>
- Nichols, J., Badman, S. V., Bagenal, F., Bolton, S., Bonfond, B., Bunce, E., et al. (2017). Response of Jupiter’s auroras to conditions in the interplanetary medium as measured by the Hubble Space Telescope and Juno. *Geophysical Research Letters*, *44*, 7643–7652. <https://doi.org/10.1002/2017GL073029>
- Nichols, J., Bunce, E., Clarke, J. T., Cowley, S., Gérard, J. C., Grodent, D., & Pryor, W. R. (2007). Response of Jupiter’s UV auroras to interplanetary conditions as observed by the Hubble Space Telescope during the Cassini flyby campaign. *Journal of Geophysical Research*, *112*, A02203. <https://doi.org/10.1029/2006JA012005>
- Radioti, A., Grodent, D., Gérard, J. C., Bonfond, B., & Clarke, J. (2008). Auroral polar dawn spots: Signatures of internally driven reconnection processes at Jupiter’s magnetotail. *Geophysical Research Letters*, *35*, L03104. <https://doi.org/10.1029/2007GL032460>
- Russell, C., Khurana, K., Huddleston, D., & Kivelson, M. (1998). Localized reconnection in the near Jovian magnetotail. *Science*, *280*(5366), 1061–1064. <https://doi.org/10.1126/science.280.5366.1061>
- Shukhtina, M., Dmitrieva, N., & Sergeev, V. (2014). On the conditions preceding sudden magnetotail magnetic flux unloading. *Geophysical Research Letters*, *41*, 1093–1099. <https://doi.org/10.1002/2014GL059290>
- Tao, C., Kataoka, R., Fukunishi, H., Takahashi, Y., & Yokoyama, T. (2005). Magnetic field variations in the Jovian magnetotail induced by solar wind dynamic pressure enhancements. *Journal of Geophysical Research*, *110*, A11208. <https://doi.org/10.1029/2004JA010959>
- Vasyliunas, V. (1983). *Plasma distribution and flow*. In A. J. Dessler (Eds.), 395–453. New York: Cambridge University Press. <https://doi.org/10.1017/CBO9780511564574.013>
- Vogt, M. F., Jackman, C. M., Slavin, J. A., Bunce, E. J., Cowley, S. W., Kivelson, M. G., & Khurana, K. K. (2014). Structure and statistical properties of plasmoids in Jupiter’s magnetotail. *Journal of Geophysical Research: Space Physics*, *119*, 821–843. <https://doi.org/10.1002/2013JA019393>
- Vogt, M. F., Kivelson, M. G., Khurana, K. K., Joy, S. P., & Walker, R. J. (2010). Reconnection and flows in the Jovian magnetotail as inferred from magnetometer observations. *Journal of Geophysical Research*, *115*, A06219. <https://doi.org/10.1029/2009JA015098>
- Woch, J., Krupp, N., & Lagg, A. (2002). Particle bursts in the Jovian magnetosphere: Evidence for a near-Jupiter neutral line. *Geophysical Research Letters*, *29*(7), 1138. <https://doi.org/10.1029/2001GL014080>
- Yao, Z. (2017). Observations of loading-unloading process at Saturn’s distant magnetotail. *Earth and Planetary Physics*, *1*(1), 53–57. <https://doi.org/10.26464/epp2017007>
- Yao, Z., Radioti, A., Grodent, D., Ray, L. C., Palmaerts, B., Sergis, N., et al. (2018). Recurrent magnetic dipolarization at Saturn: Revealed by Cassini. *Journal of Geophysical Research: Space Physics*, *123*, 8502–8517. <https://doi.org/10.1029/2018JA025837>
- Yoshioka, K., Murakami, G., Yamazaki, A., Tsuchiya, F., Kagitani, M., Sakanoi, T., et al. (2013). The extreme ultraviolet spectroscopy for planetary science, EXCEED. *Planetary and Space Science*, *85*, 250–260. <https://doi.org/10.1016/j.pss.2013.06.021>